Measurement of the high-temperature strain of UHTC materials using chemical composition gratings

Weihua Xie[1], Songhe Meng[1], Hua Jin[1*], Chong Du[2], Libin Wang[1], Tao Peng[1], F. Scarpa[3] and Shiyu Huo[1]

[1] Centre for Composite Materials and Structures, Harbin Institute of Technology, Harbin 150080, China

[2] Shanghai Advanced Research Institute, Chinese Academy of Sciences, Shanghai, China

[3] Advanced Composites Centre for Innovation and Science (ACCIS), University of Bristol, BS8 1TR Bristol, UK

Email: michael@hit.edu.cn, mengsh@hit.edu.cn, Jinhua2007@hit.edu.cn, duc@sari.ac.cn, wanglibin_hit@163.com, boypengtao@163.com, F.Scarpa@bristol.ac.uk and huoshiyu2008@126.com

Abstract

This paper proposes a simple bonding and measuring technique to realise silica-based chemical composition gratings' (CCGs) high temperature applications on hot structures. We describe a series of experiments on CCGs to measure the thermal and mechanical response characteristics of ultra-high temperature ceramic (UHTC) materials when the maximum temperature is above 1000°C. Response characteristics are obtained at the heating and cooling stages. Results show that the wavelength response of the CCGs bonded on the UHTC plate increases non-linearly with increasing temperatures, but decreases almost linearly with decreasing temperatures. The temperature-dependent strain transfer coefficients are calculated theoretically and experimentally; results show that the values of strain transfer coefficients below 1000°C are significantly affected by the thermal expansion coefficient of the substrate material and the interface. The strain transfer coefficient value tends to vary slowly between 0.616 and 0.626 above 700°C.

Keywords： Fibre optics sensors; Chemical composition gratings; High-temperature application; Ultra-high temperature ceramics; Strain and temperature;

1. Introduction

Future aerospace and spacecraft developments require a step change in high-temperature measuring technologies, in particular concerning the development of re-entry and hypersonic vehicles. At present the service temperature of thermal protection systems (TPS) and related hot structures is generally higher than 1000°C. Advanced materials like ultra-high-temperature ceramics (UHTCs), C/C and C/SiC are being rapidly developed, and are showing significant potential for aerospace applications in demanding environments [1]. Especially UHTCs made from high-melting borides, carbides and oxides have undergone significant developments because of their excellent oxidation resistance above 2000°C. However, the technology associated with experimental techniques for measuring the mechanical response of these materials at extremely high temperatures is still open to improvements. The lack of high-quality data related to the high-temperature thermo-mechanical behaviour of materials and structures in realistic operational conditions limits both the design and the structural

[1] Corresponding author: Dr. Hua Jin, Centre for Composite Materials and Structures, Harbin Institute of Technology, Harbin 150080, China. Email: jinhua2007@hit.edu.cn

integrity of vehicles, and undetected damage to or failure of TPS can lead to catastrophe [2] – as shown by the two Space Shuttle disasters.

In the last two decades, a lot of Fibre Bragg Gratings (FBGs)-based sensors have been developed for application in high-temperature environments, such as type I gratings, type II gratings, long-period gratings, photonic crystal fibres, sapphire gratings, and Chemical Composition Gratings (CCGs), now commonly called Regenerated FBGs (RFBGs). Although we can categorise these high-temperature sensors into several kinds, all of them have the same intrinsic advantages, including configurability, strong electromagnetic compatibility, lightweight, small size, good heat resistance and long-distance transmission capabilities. Some of the most recent and promising silica-based FBGs are the so-called RFBGs. RFBGs are created typically in hydrogen loaded optical fibres by applying an annealing treatment at temperatures between 800°C and 1000°C[3]. The original grating is completely erased, and a new grating refractive index modulation that can withstand temperatures up to 1295°C [4] is created during the annealing process. The main advantages of RFBGs compared with other optical sensing techniques are its ultrahigh temperature stability, good grating qualities, the possibility of measuring reflected light, and multiplexing capability. These characteristics make the regenerated gratings technique attractive to high-temperature sensing applications.

CCGs were first presented as typical RFBGs by M. Fokine et al. [5] in 2002. They fabricated several kinds of CCGs by periodically changing the concentration of fluorine [5-7], the different dopants [8], and later the concentration of oxygen [9] in the fibre core. B. Zhang et al. [10; 11] reported a novel high-temperature-resistant FBG temperature sensor in 2007; its refractive index is formed by a periodic modulation of molecular water inside the fibre core. A number of different mechanisms, such as the seeded crystallisation model, were proposed by J. Canning et al. [4; 12-14] in 2008 to explain the mechanism of thermal regeneration. In order to improve the grating properties and their thermal reliability, D. Barrera [15-17], B. Guan [18-20] and other researchers [21-25] engaged in further studies, including on tailoring the glass composition, pre-processing, the formation of gratings, and laser technologies. Bueno et al. [3] provide a very effective method to fast regenerate the FBG for high-temperature applications. With this method the treatment time can be reduced from up to an hour to several minutes or even seconds, which makes easier the application of RFBGs. However, the understanding of the mechanisms underlying the grating regeneration is still limited, and different opinions on the matter do exist [26-28]. Recently, Fokine et al. [29] found new evidence to support their point of view of about the mechanisms in place, although the practical applications of FBGs are not substantially affected by the uncertainty associated to the grating generation.

The exposure of silica-based RFBGs to high temperature during the annealing process makes them brittle and fragile, and they lose almost all of their mechanical strength [30]. For usage of silica-based RFBGs in high-temperature environments, an important problem is represented by sensor packaging and installation. A number of researchers have begun to concentrate efforts on the practical aspects of using RFBGs in high-temperature structures. Latini et al. [2; 31] developed a prototype for a structural health monitoring (SHM) system using high-temperature-resistant FBG sensors to measure temperature, and using a silica-sapphire-based extrinsic Fabry–Perot interferometric (EFPI) sensor to measure strain with working temperature up to 800°C. Méndez [32; 33] and Selfridge et al. [34] mounted CCGs onto a metal shim using a silica-filled epoxy compound, providing a pre-packaged FBG sensor that can be spot-welded onto a hot metal structure up to 800°C. Reddy [35] and Barrera et al. [36-38] provide a good way to encapsulate RFBGs with a metal tube or a combination of ceramic and metal tubes, which can be used to measure temperatures up to 1100°C. R.L.N.S. Prasad et al. [39; 40] glued CCGs onto the surface of a metal plate, providing a useful simulation and experimental method to measure the temperature (up to 900°C) and strain response of a metal structure; the most suitable material to encapsulate the FBG for temperature sensing was also studied. Azhari et al. [41] developed a simple optical sensor based on conventional FBGs using yttria-stabilised zirconia tubes, which can be used to measure the temperature up to 1100°C.

This paper seeks to solve some aspects associated to the practical technology of these optical fibre sensors by using a type of adhesive to connect the RFBGs to the structure. This particular bonding technique guarantees that the RFBGs are sensitive not only to the temperature but also to the strain level occurring in the structures with respect to the optical fibre sensors encapsulated in the tube. The technique described in this paper offers a real advantage compared to commonly established procedures, because most of the encapsulated sensors [35-40] can only be used to measure the temperature of the environments but have difficulties to measure the strain in hot structures. We also present a simple thermo-mechanical measurement method suitable for application on hot structures made of UHTCs based on CCGs, together with a decoupling technique to separate temperature and strain effects. The relation between the strain transfer coefficient and the test data is also analysed as a function of the change in the CCGs and adhesion properties at high temperatures. The thermo-mechanical characteristics of the CCGs are determined from tests carried out on UHTC material specimens. The sensor bonding and measuring technique proposed in this paper combines simultaneous temperature and strain measurement in the structure, and allows the monitoring of the mechanical and thermal behaviour of UHTCs above the thousands of degrees.

2. Experimental layout

In previous experiments carried out in L-shaped specimens the sensor was attached to the horizontal section, and the vertical section of the L-shaped sample was hit by laser [42-44]. It is difficult however to achieve a stable control of the laser heating process above 800 °C, and in this work the heating process and the shape of the specimens are changed.

The improved experimental rig is shown in Figure 1, with the laser heater vertically mounted at the bottom of the gantry. The laser beam is emitted through the reserved laser heating hole from the lower side. The plate specimen is mounted on the hole of the test table and the FBG sensor is attached to the surface of the specimen. The CCGs used in this study was fabricated with Ge-doped silica fibres in the Institute of Photonics Technology (Jinan University, China). The experimental setup shown in figure 1 allows a rapid heating of the specimen along its thickness direction.

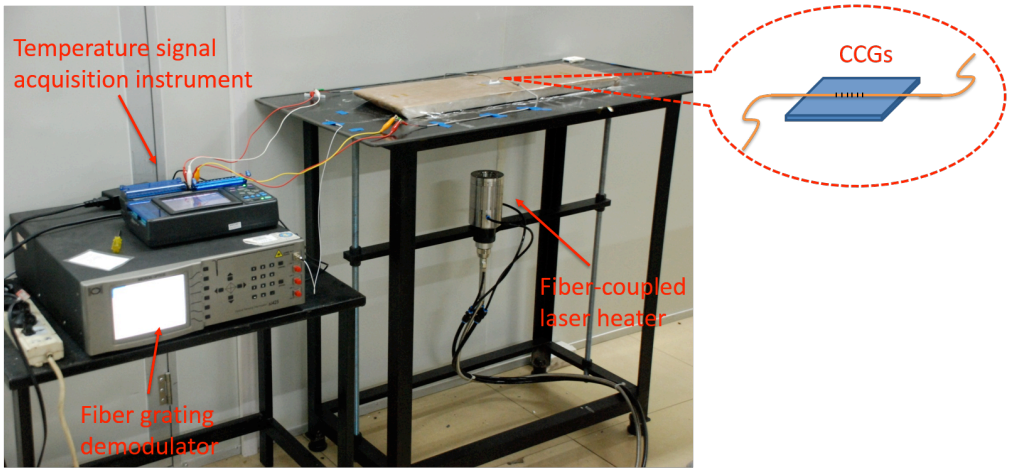

Figure 1. Experimental rig for the CCGs high-temperature test

The experiment makes use of a high-power fibre-coupled laser for heating (DILAS Diodenlaser GmbH, Germany. Laser class: Compact-980.10-1500C, Output power: 1500W, Wavelength: 980nm±10nm@25°C). To simulate a realistic heating condition existing of the outer surfaces of airframes or spaceframes [2; 45], the specimen located above the opening region is heated vertically from the bottom The diameter of the heating spot is 20mm, and the

distance from the heating lens to the specimen is 200mm. Due to the extremely high thermal conductivity of the UHTC, the heat is quickly transmitted from the lower side of the rig. The reflected wavelengths are acquired from the optical fibre grating demodulator (si425 Optical Sensing Interrogator, Micron Optics, Inc., USA). Meanwhile, the temperature response from a thermocouple is recorded by a multi-channel temperature signal acquisition instrument (LR8402-21, HIOKI, Japan). During the test, the laser heating lens is moved vertically and horizontally by adjusting a screw gear at the bottom of the laser heater. The overall temperature increasing rate of the specimen is controlled with the adjustment of the laser heater output power combined with the temperature response data.

3. Strain transfer characteristics of CCGs bonding on UHTCs

3.1 The concept of strain transfer coefficient

Figure 2 shows a schematic diagram of the positions of the UHTCs structure, the adhesive and the CCGs, which is applied near the structure surface. The strain of the substrate material caused by heat or mechanical loading is transmitted to the grating in the form of a surface shear stress through the adhesive layer made from a high purity alumina adhesive (Rebond 989FS, COTRONICS CORP., USA). Because of the contribution of the adhesive layer absorption to stress and deformation, there is a difference between the grating and the actual sensed strains that can be represented by a strain transfer coefficient β between the measured strain and the true strain. This coefficient directly depends upon the material of the structure, the physical characteristics of the adhesive and the geometry/size of the colloid used. It is possible to identify the values of the strain transfer coefficient from the experimental test data.

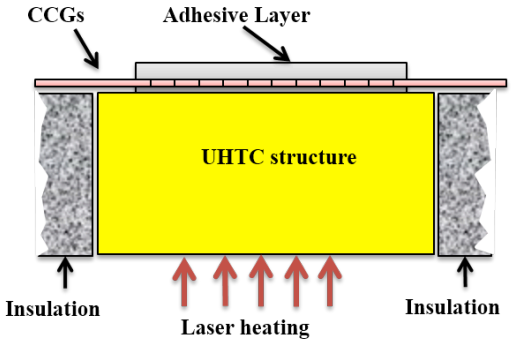

Figure 2. A scheme illustrating the physics of the strain transfer.

3.2 The relation between the strain transfer coefficient and the test data

Temperature compensation is usually adopted to decouple CCGs signals [46] by installing a thermocouple at the same measurement location to measure the temperature response of the grating. The thermocouple signal is used to eliminate the CCGs response wavelength caused by the temperature variation. The wavelength response measured at specific temperatures is calculated taking into account the sensitivity between the CCGs and the temperature. When the wavelength drift caused by the temperature variations is removed from the overall signal the remaining part of the wavelength is related to strain measurements. The assumption behind the decoupling is that no cross-influence between temperature and strain in the considered wavelengths and temperature ranges do however exist.

Equation (1) describes the CCGs response signal change measured during the experiment:

$$\Delta\lambda_B = \Delta\lambda_T + \Delta\lambda_\varepsilon \tag{1}$$

The amount of change in the wavelength of the CCGs versus the temperature variations is denominated as $\Delta\lambda_T$. This quantity usually depends upon the thermal expansion coefficient

and the thermo-optical effects existing in the substrate materials, and on the CCGs center wavelength [30]. The amount of changes in the wavelength of the CCGs for the strain corresponds to $\Delta\lambda_\varepsilon$, and it is affected by the strain and wavelength of CCGs, as well as the elastic-optic effect [47]. The theoretical relation of the strain sensitivity coefficient K_ε with the center wavelength λ_B and the strain variation $\Delta\varepsilon$ is [42; 48]:

$$\Delta\lambda_\varepsilon = K_\varepsilon \lambda_B \Delta\varepsilon = \left(1 - P_e\right)\lambda_B \Delta\varepsilon \tag{2}$$

Where P_e=0.22 is the effective elastic-optic coefficient.

When the material substrate bonded to the CCGs experiences no mechanical loading at high temperature the total thermal strain includes the thermal strain of the substructure and the thermal strain of the CCGs itself. The global strain can be represented by the actual strain from the CCGs measurement multiplied by a factor β [43]:

$$\Delta\varepsilon = \beta(\alpha_s - \alpha)\Delta T \tag{3}$$

In equation (3), α_s denotes the thermal expansion coefficient of substrate material and α is associated to the thermal expansion coefficient of the CCGs.

To calculate the effect of the thermal strain on the wavelength, it is possible to derive from equations (2) and (3) the following relation [43]:

$$\Delta\lambda_\varepsilon = K_\varepsilon \lambda_B \Delta\varepsilon = K_\varepsilon \lambda_B \beta\left(\alpha_s - \alpha\right)\Delta T \tag{4}$$

When a high temperature response test is carried out with the CCGs bonded to the substrate, the relative variation of the measured total wavelength response can be further represented as a quadratic equation of temperature variations [43]:

$$\frac{\Delta\lambda_B}{\lambda_B} = \frac{\Delta\lambda_T + \Delta\lambda_\varepsilon}{\lambda_B} = K_{T1}\Delta T + K_{T2}\Delta T^2 + C \tag{5}$$

Where K_{T1} and K_{T2} represent the first- and second-order sensitivity coefficient respectively, and C is a universal constant.

The wavelength drift caused by the temperature variations can be written in the form of a quadratic [16; 17] function:

$$\Delta\lambda_T = \lambda_B(C_1 + (\alpha + \zeta)\Delta T + \frac{1}{2}(\alpha^2 + \zeta^2 + 2\alpha\zeta + \frac{\partial\alpha}{\partial T} + \frac{\partial\zeta}{\partial T})\Delta T^2) \tag{6}$$

Where ζ is the thermo-optical coefficient of the CCGs, and C_1 is another universal constant. We can substitute equations (4) and (6) into equation (5), then we can get the first-order sensitivity coefficient K_{T1}:

$$K_{T1} = \left(\alpha + \zeta\right) + K_\varepsilon \beta\left(\alpha_s - \alpha\right) \tag{7}$$

The parameter K_{T1} contains the effects of both the temperature changes on the CCGs itself and the strain provided by the thermal expansion of the structure that is caused by the temperature acting on the CCGs. K_{T1} can be known by calculating the values from the experimental data. Then from equation (7) it is possible to obtain the strain transfer coefficient β as a function of the temperature T:

$$\beta(T) = \frac{K_{T1} - \left(\alpha + \zeta\right)}{K_\varepsilon(\alpha_s(T) - \alpha)} \tag{8}$$

4. Temperature and strain response characteristics of a test on a UHTCs

4.1 High temperature experimental test

The high temperature experimental test is performed using two different types of CCGs with center wavelengths of 1540nm and 1553nm. The installation of the UHTCs and CCGs is shown in figure 3(a). The UHTCs samples for the tests were fabricated from commercial ZrB_2 (Northwest Institute for Non-ferrous Metal Research, China) and SiC powders (Weifang Kaihua Micro-powder Co. Ltd., China). The powder mixtures of ZrB_2 with 15% v/v SiC were ball milled in ethanol for 8 hours with a hard milling tool, and dried in a rotating evaporator. Milled powder was then uniaxial hot pressed in a boron nitride coated graphite die at 1950°C for 60 min under vacuum and 30MPa of applied pressure. Because of the specimen's thickness (40mm×45mm×5mm), an insulation package is placed around the specimen to provide both support and insulation. The specimen is embedded in the insulating body, therefore the surface of the specimen and the thermal isolation are on the same work plane. It is possible to note the circular area below which the laser heating occurs (figure 3(b)).

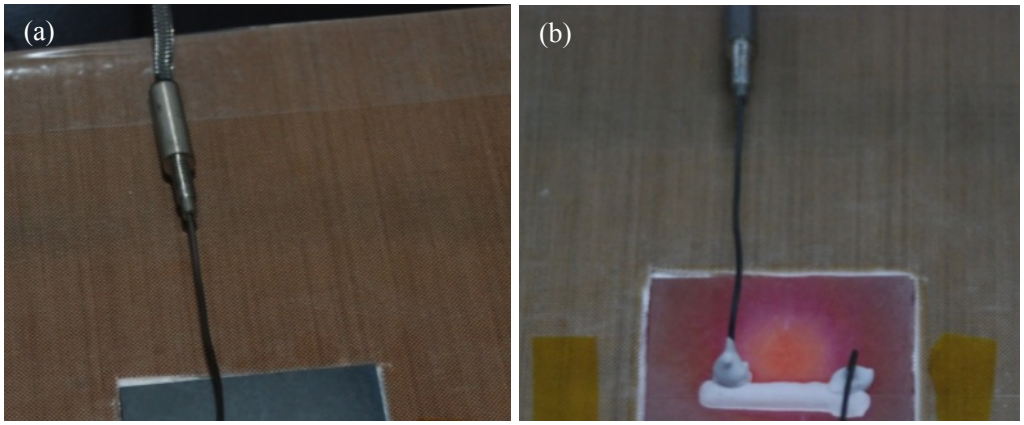

Figure 3. Images of the UHTCs specimen (a) before experiment and (b) during high temperature test

4.2 High temperature experiment data at 1000°C

The highest temperature recorded during the test is 1006°C for the CCGs with the 1540nm center wavelength. The curve of the measured response signals of the CCGs versus the temperature is shown in figure 4. It is possible to observe that the response of the wavelength presents a nonlinear increase for rising temperatures. The nonlinearity is induced by the highly temperature-dependent of thermo-optical coefficient and the thermal expansion coefficient of the silica fibre [49], it's also affected by the change period of the fibre and elastic-optic coefficient [50], hence the response exhibits a non-linearity. The wavelength maintains a steady upward trend except for some small sinusoidal fluctuations around 500°C. This variation is similar to the wavelength drift of regeneration process shown in the curve in figure6 (b) of reference [51].

Figure 5(a) shows the results from the quadratic curve fitting of the wavelength relative variation versus temperature, and table 1 lists the curve fitting parameters with 95% confidence interval and R^2=0.992. The similar quadratic thermal responses were observed at literature [16; 17; 52; 53]. The parameter K_{T1} is the one identified from the quadratic curve fitting, and it can used to calculate the strain transfer coefficient β from equation (8). After the strain transfer coefficient is obtained, the strain variation of the specimen and the relative variation of the wavelength can be calculated by using equations (3) and (2) respectively. Figure 5(b) shows the relation between variation of the relative wavelength response and the thermal strain of the specimen. According to reference [43], the temperature dependence of the material substrate could not be considered. However, the thermal expansion coefficient of

the UHTCs obviously changes within a larger temperature range (figure 6), and therefore in this paper, the dependence of the coefficient of thermal expansion related to the substrate material thermal expansion is taken into account. The calculated strain transfer coefficients at different temperatures are shown in table 2. The coefficients range from 0.616 to 0.909, and their values decrease gradually with increasing temperature rising. These data clearly indicate that the thermal expansion coefficient of the substrate material has an obvious effect on the strain transfer coefficient.

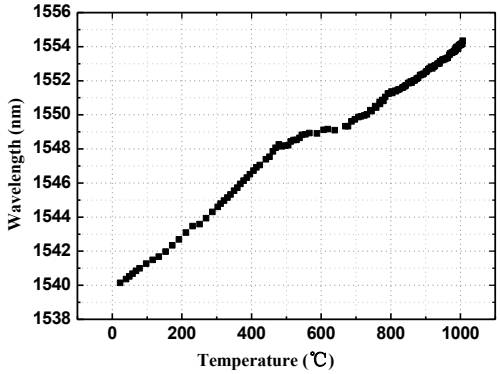

Figure 4. Wavelength variation of the CCGs sensor up to 1000°C.

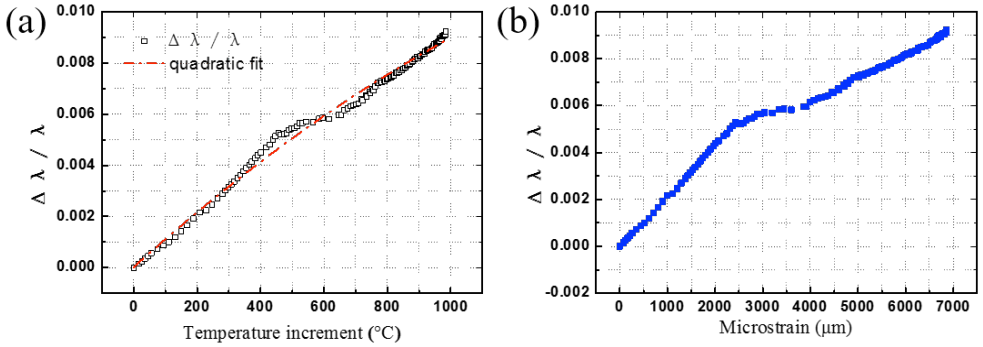

Figure 5. Relative variation of wavelength (1000°C). (a) With temperature. (b) With thermal strain.

Table 1. Fitting parameters of experiments data up to 1000°C

Parameter	Value	Standard deviation
K_{T1}	1.09549E-5	3.13599E-7
K_{T2}	-2.03681E-9	2.74332E-10
C	8.51364E-5	7.74032E-6

Table 2. Strain transfer coefficient of 1000°C experiments

Temperature (°C)	200	300	400	500	600	700	800	900	1000
β	0.909	0.892	0.781	0.778	0.685	0.632	0.633	0.619	0.616

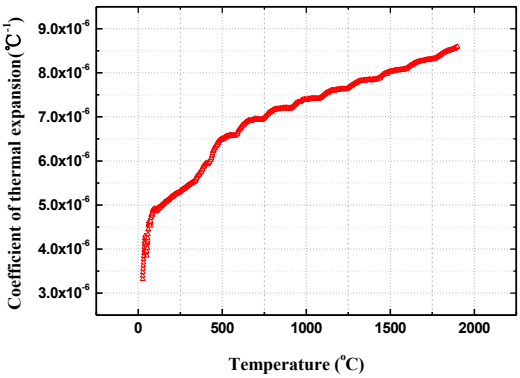

Figure 6. Coefficient of thermal expansion of the UHTCs with temperature.

4.3 Experiments at 800°C

To compare the response of CCGs with different center wavelengths, a test has been initially carried out first with CCGs sensors with a center wavelength of 1553nm (800°C). The maximum peak temperature when heating has been set at 800°C, although an actual peak temperature of 810°C has been measured. Once the temperature reaches the peak it then slowly decreases by decreasing the output power lased and leaving the sample to cool. The response signals during the cooling process recorded at the same time.

The relation between the wavelength response and the temperatures is shown in figure 7. The wavelength maintains a steady nonlinear increase in the temperature-rise zone except for small sinusoidal fluctuations around 500°C. However, the line corresponding to the temperature decrease has a more linear behavior, which is quite different from the one of the heating phase. The whole process has some qualitative similarities (in terms of shape of the curves) with the work hardening behavior present in some high point melting metals. The variation of the response of the CCGs during the temperature decrease is due to the equivalent plastic deformation of the adhesive-CCGs-substrate in a high-temperature environment.

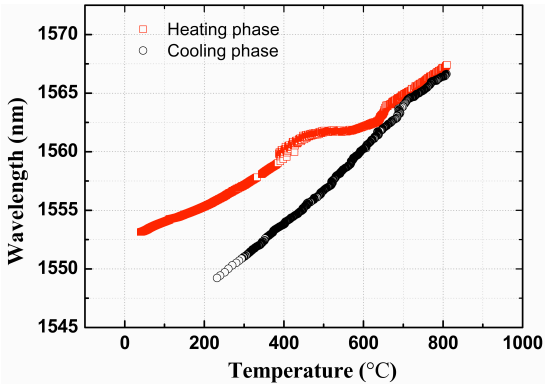

Figure 7. Wavelength variation of the sensor at 800°C.

Figure 8(a) describes the relative variation of the wavelength response in the UHTCs specimen for increasing temperatures with the quadratic fitting of equation (8) and related parameters with 95% confidence interval shown in table 3. Similarly to the derivation of data in figure 5(b), the same calculation process was used to compute the strain variation of the specimen and the relative variation of the wavelength. Figure 8(b) shows the relationship between the wavelength relative variation of the specimen and the thermal strain. From the

qualitative point of view, it is possible to notice that the curves assume similar shapes and trends.

Table 3. Fitting parameters of experiments data up to 800°C

Parameter	Heating phase (R^2=0.989)		Cooling phase (R^2=0.998)	
	Value	Standard deviation	Value	Standard deviation
K_{T1}	1.10688E-5	1.28442E-7	1.57092E-5	2.54105E-7
K_{T2}	8.07737E-10	1.58066E-10	4.84547E-9	2.45335E-10
C	-1.89162E-4	2.07932E-5	-0.00592E-0	6.19948E-5

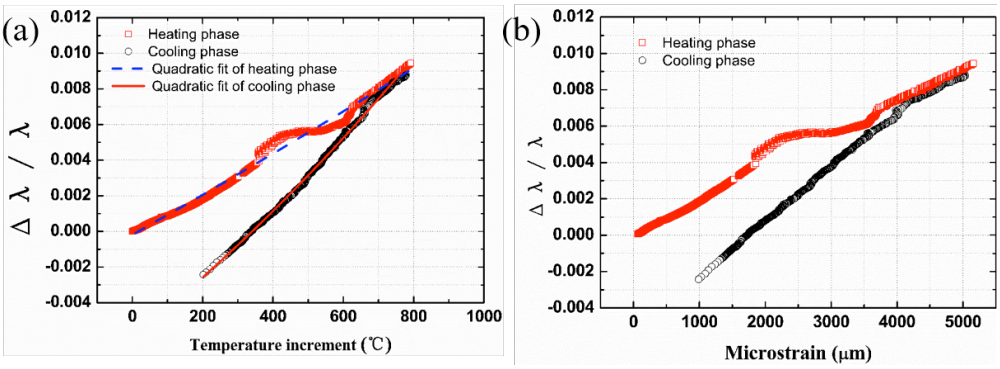

Figure. 8. Relative variation of the wavelength at 800°C versus (a) temperature and (b) thermal strain.

4.4. Analysis of the high temperature experimental results

From the previous observations of Figs. 5(a) and 8(a) it is possible to note that the wavelength data tend to fluctuate at about 500°C. One reason for this behavior is that when the steady-state temperature of the specimen and the adhesive reaches approximately 500°C, the inner microstructure of the adhesive layer begins to change, as part of the adhesive has softened at this temperature level. This change in microstructure leads to a change of the interface state between the adhesive and the CCGs, as well as between the adhesive and the UHTC material. The consequence of these changes in interface behavior significantly affects the strain transfer of the specimen to the CCGs, and therefore the CCGs signals will fluctuate.

When one compares the calculated strain transfer coefficient at 800°C with the test data at 1000°C and the one reported in reference [43] (see figure 9) it is possible to notice that the strain transfer coefficient will decrease for increasing temperature. The coefficient however presents a stable trend after 700°C, with a value between 0.616 and 0.626. The deviation of the test data under different conditions is mainly caused by the difference in the CCGs center wavelengths and experiment methods.

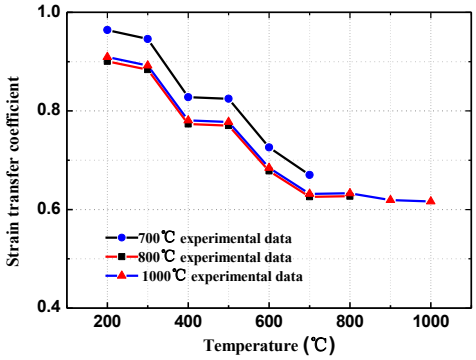

Figure 9. Comparison of the strain transfer coefficient of the UHTCs tested.

5. Conclusions

This work has described the bonding and manufacturing of a high temperature strain measurement system based on CCGs. The response characteristics of the bonded CCGs from room temperature to 1000°C are revealed by a signal decoupling technique on the basis of a temperature compensation method. Because of the effect of the adhesive absorption in the thermal structural strain response, a formula to calculate a specific strain transfer coefficient has also been developed. The temperature response test is carried out on a UHTC material, and the results indicate that the wavelength response signal increases non-linearly with increasing temperatures. In particular, the strain transfer coefficient value is significantly affected by the thermal expansion coefficient, but remains stable above 700°C. This paper provides a simple method to apply silica-based optical fibre sensors on practical aerospace structures to measure strain at high temperatures up to 1000°C. However, further investigations are needed to discover the mechanism of sinusoidal fluctuations around 500°C.

Acknowledgments

This research was supported by the Project of Natural Science Foundation of China (11272107, 11472092 and 11502058), National Basic Research Program of China (2015CB655200). The authors thank Institute of Photonics Technology (Jinan University, Guangzhou, China) for providing the CCGs sensors.

References

[1] Glass D E 2008 Ceramic matrix composite (CMC) thermal protection systems (TPS) and hot structures for hypersonic vehicles. In: *15th AIAA space planes and hypersonic systems and technologies conference,* pp 1-36

[2] Latini V, Striano V, Coppola G and Rendina I 2007 Fiber optic sensors system for high-temperature monitoring of aerospace structures. In: *Microtechnologies for the New Millennium*: International Society for Optics and Photonics) pp 65930S-S-9

[3] Bueno A, Kinet D, Mégret P and Caucheteur C 2013 Fast thermal regeneration of fiber Bragg gratings *Opt Lett* **38** 4178-81

[4] Canning J, Stevenson M, Bandyopadhyay S and Cook K 2008 Extreme Silica Optical Fibre Gratings *Sensors* **8** 6448-52

[5] Fokine M 2002 Thermal stability of chemical composition gratings in fluorine–germanium-doped silica fibers *Opt Lett* **27** 1016-8

[6] Fokine M 2002 Photosensitivity, chemical composition gratings and optical fiber based components

[7] Fokine M 2002 Formation of thermally stable chemical composition gratings in optical fibers *JOSA B* **19** 1759-65

[8] Pal S, Mandal J, Sun T, Grattan K, Fokine M, Carlsson F, Fonjallaz P Y, Wade S and Collins S 2003 Characteristics of potential fibre Bragg grating sensor-based devices at elevated temperatures *Measurement Science and Technology* **14** 1131
[9] Fokine M 2004 Thermal stability of oxygen-modulated chemical-composition gratings in standard telecommunication fiber *Opt Lett* **29** 1185-7
[10] Zhang B 2007 *Optical high temperature sensor based on fiber Bragg grating*
[11] Zhang B and Kahrizi M 2007 High-temperature resistance fiber Bragg grating temperature sensor fabrication *Sensors Journal, IEEE* **7** 586-91
[12] Bandyopadhyay S, Canning J, Stevenson M and Cook K 2008 Ultrahigh-temperature regenerated gratings in boron-codoped germanosilicate optical fiber using 193 nm *Opt Lett* **33** 1917-9
[13] Canning J, Cook K, Aslund M, Stevenson M, Biswas P and Bandyopadhyay S 2010 *Regenerated fibre Bragg gratings*: INTECH Open Access Publisher)
[14] Canning J, Stevenson M, Fenton J, Aslund M and Bandyopadhyay S 2009 Strong regenerated gratings. In: *20th International Conference on Optical Fibre Sensors*: International Society for Optics and Photonics) pp 750326--4
[15] Barrera D 2010 Fiber-optic sensors for high-temperature applications *SPIE Newsroom* **6**
[16] Barrera D, Finazzi V, Coviello G, Bueno A, Sales S and Pruneri V 2010 Chemical composition gratings in Germanium doped and Boron-Germanium co-doped fibers. In: *SPIE Photonics Europe*: International Society for Optics and Photonics) pp 772607--7
[17] Barrera D, Finazzi V, Villatoro J, Bueno A, Sales S and Pruneri V 2010 On the use of Optical Fiber Sensors (CCGs and PCFI) for Harsh Environments
[18] Li G and Guan B-o 2010 Research on reflectivity of chemical composition grating sensors at high temperatures. In: *Asia Communications and Photonics Conference and Exhibition*: International Society for Optics and Photonics) pp 79860U-U-5
[19] Li G and Guan B o 2011 Improvement on reflectivity of chemical composition gratings at high temperatures *Microw Opt Technol Let* **53** 963-6
[20] Li G, Liu M, Li Y and Guan B o 2012 Fabrication and sensing characteristics of the chemical composition grating sensor at high temperatures *Microw Opt Technol Let* **54** 71-5
[21] Cheong Y, Chong W, Chong S, Lim K and Ahmad H 2014 Regenerated Type-IIa Fibre Bragg Grating from a Ge–B codoped fibre via thermal activation *Optics & Laser Technology* **62** 69-72
[22] Coviello G, Finazzi V, Villatoro J and Pruneri V 2009 Thermally stabilized PCF-based sensor for temperature measurements up to 1000ºC *Opt Express* **17** 21551-9
[23] Grobnic D, Smelser C W, Mihailov S J and Walker R B 2006 Long-term thermal stability tests at 1000 C of silica fibre Bragg gratings made with ultrafast laser radiation *Measurement Science and Technology* **17** 1009
[24] Laffont G, Cotillard R and Ferdinand P 2012 Multiplexed regenerated fiber Bragg gratings for high temperature measurement. In: *OFS2012 22nd International Conference on Optical Fiber Sensor*: International Society for Optics and Photonics) pp 842123--4
[25] Lindner E, Canning J, Chojetzki C, Brückner S, Becker M, Rothhardt M and Bartelt H 2011 Thermal regenerated type IIa fiber Bragg gratings for ultra-high temperature operation *Opt Commun* **284** 183-5
[26] Canning J, Bandyopadhyay S, Stevenson M, Biswas P, Fenton J and Aslund M 2009 Regenerated gratings *Journal of the European Optical Society-Rapid publications* **4**
[27] Cook K, Shao L-Y and Canning J 2012 Regeneration and helium: regenerating Bragg gratings in helium-loaded germanosilicate optical fibre *Optical Materials Express* **2** 1733-42
[28] Fokine M 2004 Underlying mechanisms, applications, and limitations of chemical composition gratings in silica based fibers *J Non-cryst Solids* **349** 98-104
[29] Holmberg P, Laurell F and Fokine M 2015 Influence of pre-annealing on the thermal regeneration of fiber Bragg gratings in standard optical fibers *Opt Express* **23** 27520-35

[30] Mihailov S J 2012 Fiber Bragg grating sensors for harsh environments *Sensors* **12** 1898-918
[31] Latini V, Striano V, Monteverde F, Rendina I and Parolini C 2010 DEDALO: Application of Structural Health Monitoring Systems on UHTC Structures *Open Aerospace Engineering Journal* **3** 32-40
[32] Méndez A, Wnuk V P, Fokine M, Claesson Å, Nilsson L-E, Ferguson S and Graver T 2005 Packaging process of fiber Bragg grating strain sensors for use in high-temperature applications. In: *Optics East 2005*: International Society for Optics and Photonics) pp 60040E-E-7
[33] Wnuk V P, Méndez A, Ferguson S and Graver T 2005 Process for mounting and packaging of fiber Bragg grating strain sensors for use in harsh environment applications. In: *Smart Structures and Materials*: International Society for Optics and Photonics) pp 46-53
[34] Selfridge R H, Schultz S M, Lowder T L, Wnuk V P, Méndez A, Ferguson S and Graver T 2006 Packaging of surface relief fiber Bragg gratings for use as strain sensors at high temperature. In: *Smart Structures and Materials*: International Society for Optics and Photonics) pp 616702--7
[35] Reddy P S, Prasad R L N S, Gupta D S, Shankar M S, Narayana K S and Kishore P 2011 Encapsulated fiber Bragg grating sensor for high temperature measurements *Opt Eng* **50** 114401--6
[36] Barrera D, Finazzi V, Villatoro J, Sales S and Pruneri V 2011 Performance of a high-temperature sensor based on regenerated fiber Bragg gratings. In: *21st International Conference on Optical Fibre Sensors (OFS21)*: International Society for Optics and Photonics) pp 775381--4
[37] Barrera D, Finazzi V, Villatoro J, Sales S and Pruneri V 2012 Packaged optical sensors based on regenerated fiber Bragg gratings for high temperature applications *Sensors Journal, IEEE* **12** 107-12
[38] Francisco García-de-Quirós J A C H, Iain McKenzie, Salvador Sales, David Barrera, Joel Villatoro, Vittoria Finazzi, Valerio Pruneri, Jesús Marcos, María Parco 2012 HiTOS: A High-Temperature Optical Fibre-based sensor system for Space structures *63rd International Astronautical Congress* **IAC-12. D1.2.9** 1-4
[39] Mamidi V R, Kamineni S, Ravinuthala L S P, Thumu V and Pachava V R 2014 Characterization of Encapsulating Materials for Fiber Bragg Grating-Based Temperature Sensors *Fiber Integrated Opt* **33** 325-35
[40] Reddy P S, Sai Prasad R L, Srimannarayana K, Sai Shankar M and Sen Gupta D 2010 A novel method for high temperature measurements using fiber Bragg grating sensor *Opt. Appl* **40** 685-92
[41] Azhari A, Liang R and Toyserkani E 2014 A novel fibre Bragg grating sensor packaging design for ultra-high temperature sensing in harsh environments *Measurement Science and Technology* **25** 075104
[42] Du C, Xie W, Meng S, Yin Y, Jiao L and Song L 2012 The connection technology based on high temperature silica fiber optic sensor. In: *SPIE Smart Structures and Materials+ Nondestructive Evaluation and Health Monitoring*: International Society for Optics and Photonics) pp 83452X-X-8
[43] Du C, Xie W, Huo S, Meng S, Xu K and Jiao L 2013 The response of high-temperature optical fiber sensor applied to different materials. In: *Fourth International Conference on Smart Materials and Nanotechnology in Engineering*: International Society for Optics and Photonics) pp 87930O-O-8
[44] S. H. Meng C D, W. H. Xie, S.Y. Huo, L.C. Jiao, H. Jin, and L.Y. Song 2013 Application of high-temperature optical fiber sensor in temperature and strain testing of hot structure *Journal of Solid Rocket Technology* **36** 701-5
[45] Manor D, Lau K Y and Johnson D B 2005 Aerothermodynamic environments and thermal protection for a wave-rider second stage *J Spacecraft Rockets* **42** 208-12

[46] Ge Y, Elshafie M Z, Dirar S and Middleton C R 2014 The response of embedded strain sensors in concrete beams subjected to thermal loading *Constr Build Mater* **70** 279-90
[47] Melle S M and Liu K 1993 Practical fiber-optic Bragg grating strain gauge system *Appl Optics* **32** 3601-9
[48] Rajan G, Ramakrishnan M, Semenova Y, Ambikairajah E, Farrell G and Peng G-D 2014 Experimental study and analysis of a polymer fiber Bragg grating embedded in a composite material *J Lightwave Technol* **32** 1726-33
[49] Li G-Y and Guan B-O 2009 The strain response of chemical composition gratings at high temperatures *Measurement Science and Technology* **20** 025204
[50] Maier R R, MacPherson W N, Barton J S, Jones J D, McCulloch S and Burnell G 2004 Temperature dependence of the stress response of fibre Bragg gratings *Measurement Science and Technology* **15** 1601
[51] Polz L, Nguyen Q, Bartelt H and Roths J 2014 Fiber Bragg gratings in hydrogen-loaded photosensitive fiber with two regeneration regimes *Opt Commun* **313** 128-33
[52] O'Dwyer M J, Ye C-C, James S W and Tatam R P 2004 Thermal dependence of the strain response of optical fibre Bragg gratings *Measurement Science and Technology* **15** 1607
[53] Trpkovski S, Kitcher D J, Baxter G W, Collins S F and Wade S A 2005 High-temperature-resistant chemical composition Bragg gratings in Er3+-doped optical fiber *Opt Lett* **30** 607-9